Data-driven sampling pattern design for sparse spotlight SAR imaging

Yao Zhao, Wenkun Huang, Xiangyin Quan, Wing-Kuen Ling and Zhe Zhang ✉

This paper proposes a joint optimization method for the imaging algorithm and sampling scheme of sparse spotlight syhthetic aperture radar (SAR) imaging based on deep convolutional neural networks. Traditional compressed sensing (CS) based sparse SAR imaging has been widely studied. Deep learning and sparse unfolding networks have been introduced into sparse SAR imaging, but most current works focus only on the imaging stage and simply adopt the conventional uniform or random down-sampling scheme. Considering that the imaging quality also depends on the sampling pattern besides the imaging algorithm, this paper introduces a learning-based strategy to jointly optimize the sampling scheme and the imaging network parameters of the reconstruction module. In a deep learning-based image reconstruction scheme, joint and continuous optimization of the sampling patterns and convolutional neural network parameters is achieved to improve the image quality. Simulation results based on real SAR image dataset illustrate the effectiveness and superiority of the proposed framework.

Introduction: As an important microwave imaging technique, synthetic aperture radar (SAR) has been widely known for its all-time, all-weather and high-resolution abilities, and has been widely used in remote sensing applications [1]. As a research focus, sparse signal processing techniques were introduced into SAR imaging since 2007 [2]. It has been shown that if the scene is sparse and the system satisfies certain constraints, the observation scene can be reconstructed with high resolution using regularization techniques, and the observation matrix of SAR systems used in the sparse recovery is constructed from the transmitted signal and the geometric relationship between the radar and the target scene. However, the empirically-chosen parameters used in canonical sparse SAR imaging methods in terms of sampling scheme, threshold and iteration stepsize and iteration times limit the imaging performance. In real applications, optimizing such parameters used to be difficult and time-consuming.

In recent years, deep network based methods have been applied to the sparse SAR imaging [3–7] tackling the reconstruction parameters including the iteration stepsize, threshold, etc for an accelerated computation. For example, Yonel et al [3] proposed a structure-specific passive SAR imaging network based on an iterative soft thresholding algorithm (ISTA). Reference [6] proposed two parametric methods for SAR super-resolution imaging based on ADMM and deep neural network. Reference [7] established a target-oriented SAR imaging method via Deep MF-ADMM-Net, which improved the signal-to-clutter ratio (SCR) of the reconstructed image. Researches show that the deep network-based approaches can reconstruct the SAR images effectively with optimized parameters learned from data. However, the above mentioned deep network based approaches does not deal with the sampling parameters, specifically, sampling schemes in the sparse SAR imaging.

In this letter, we treat the sparse spotlight SAR image recovery as an optimization problem using a deep learning prior regularization with the sampling scheme as a parameter that can be learned from data. The proposed deep network is superior to existing deep learning based sparse SAR imaging works which are simply uniformly or randomly downsampled for a sparse reconstruction. Furthermore, the presented method enables a smaller convolutional neural network architecture, making it possible to work with limited dataset size, which is usually critical in SAR imaging context.

Existing works on deep network based sparse SAR imaging usually directly inherit the canonical uniform or random down-sampling schemes. Due to the fact that the imaging quality of sparse SAR depends largely on its sampling scheme, this paper adopts a joint optimization on the sampling and imaging method. Such approach has been already applied in MRI and other fields [8]. Classical sparse SAR imaging inherits a uniform downsampling scheme, but uniform downsampling will markedly increase the ambiguity effect cased by the spectrum aliasing. State-of-the-art sparse SAR imaging methods mostly use random downsampling in order to reduce ambiguity [9]. However, random downsampling is usually not optimal, either.

In order to achieve the optimal sampling scheme, a straightforward approach is to optimize the discrete sampling locations under some specific reconstruction algorithms. This optimization problem's searching space tends to be very large and its computational complexity is usually very high. Unlike the above strategies, our work transform the discrete sampling locations into a continuous domain to reduce the searching space. Our approach also decouples the two-dimensional sampling along azimuth and range directions to two separate one-dimensional samplings, which markedly reduce the computational complexity.

SAR Imaging Model: Take the spotlight SAR system as an example, the echo of the observation scene Ω is

$$\omega(K,\theta) = \iint_{(x,y)\in\Omega} r(x,y)\exp\left\{-j2K\left(x\cos\theta + y\sin\theta\right)\right\}dxdy. \quad (1)$$

where $\omega(K,\theta)$ is the SAR echo data; $r(x,y)$ is the reflectivity function of the observation scene at location (x,y); x and y refer to the position of the range and the azimuth directions on the imaging scene; K is the wave number; and θ is the azimuth angle.

According to the projection-slice theorem, Eq. (1) can be considered as a two-dimensional Fourier transform of the scattering function. When the scene is discretized into cells in both directions and stacking the backscattering coefficients into a vector, we achieve the sparse SAR imaging model in a matrix-form

$$\omega = A_\Theta(r) + n, \quad (2)$$

where ω is the measured ehco data vector; r is the is the vector of the lexicographically ordered sparse discretised spatial scattering image of the observation area Ω; A_Θ is the compressive sensing-based SAR measurement matrix; and n is the additive noise vector of the radar system. The Θ represents the sample location when downsampling is exploited.

The 2D FFT method is very straight forward in spotlight SAR imaging, so A_Θ can be seen as the operator of 2D Fourier transform computed at the sampling locations Θ. Given Fourier data lying on a polar grid, two-dimensional interpolation techniques are used to derive values on a Cartesian grid. Once data are available on a Cartesian grid, the data are windowed and a 2D IFFT is performed to obtain spatial domain data, also on a Cartesian grid. Several techniques exist to accomplish polar-to-Cartesian reformatting [10].

Proposed Method: In this paper, we adopt a joint optimized sampling scheme and reconstruction algorithm to achieve a strong coupling between the reconstruction algorithm and the specific sampling pattern. These schemes pose the reconstruction as an optimization problem of the form

$$\hat{r}\{\Theta,\Phi\} = \arg\min_r \|\omega - A_\Theta(r)\|_2^2 + \mathcal{R}_\Phi(r). \quad (3)$$

Here $\mathcal{R}_\Phi(r)$ is a regularization penalty, and canonical regularization based algorithms are widely used for the recovery of images from heavily downsampled measurements.

Deep learning-based regularized image reconstruction: Tackling the model (2), we treat the image reconstruction as a regularization optimization scheme and use a deep learning approach instead of the traditional fixed prior regularization to learn parameters from data samples with optimization sampling scheme as

$$\hat{r}\{\Theta,\Phi\} = \arg\min_r \|\omega - A_\Theta(r)\|_2^2 + \lambda\ \|C_\Phi(r)\|_F^2\,, \quad (4)$$

where $C_\Phi(r)$ is a convolutional neuron network (CNN) used to extract the "non-ideal" components from the reconstructed SAR image. In the context of sparse SAR imaging, the "non-ideal" components usually refer to the deviation from an ideal and clean sparse SAR image , commonly consists of noise, downsampled ambiguities and other perturbations that can be suppressed by canonical shrinkage operations in traditional sparse SAR imaging. $C_\Phi(r)$ depends on the learned parameters Φ which represents the features of non-ideal components. It can be expressed as

$$C_\Phi(r) = (I - D_\Phi)(r) = r - D_\Phi(r), \quad (5)$$

where D_Φ is a network to remove the non-ideal components from the image. That is, if r is contaminated with non-ideal components, the $\|C_\Phi(r)\|_F^2$ tends to be large hence yields a solution with minimal non-ideal components. λ here is a trainable regularization parameter

to balance the fidelity term $\|\omega - A_\Theta(r)\|_2^2$ and the regularization term $\|C_\Phi(r)\|_F^2$.

The above optimization problem can be solved using an iterative algorithm that alternates between a data consistency step and a denoising step.

$$r_{n+1} = (A_\Theta^H A_\Theta + I)^{-1}(z_n + A_\Theta^H \omega), \tag{6}$$

$$z_{n+1} = D_\Phi(r_{n+1}). \tag{7}$$

The algorithm is initialized with $z_0 = 0$. The proposed method is shown in Figure 1. Unfolding the canonical iterative Eqs. (6-7), we obtain a deep recursive network $M_{\Theta,\Phi}$.

The framework alternates between a data consistency block Q_Θ and a denoising block D_Φ. The data consistency block Q_Θ works as the fidelity term in (4) as defined in Eq. (6). It depends only on the sampling pattern. The denoising block D_Φ works as the regularization term in (4) to remove the non-ideal components, which is a convolutional neural network.

When z_n is initialized, Q_Θ inverts the measured Fourier samples. In this paper, Q_Θ is implemented by the conjugate gradient algorithm. Q_Θ and weights of the CNN block D_Φ keep invariant during the iteration and are shared by each unfolded layer.

Therefore, the solution to above optimization problem can be given by

$$\hat{r}\{\Theta, \Phi\} = M_{\Theta,\Phi}(A_\Theta(r)), \tag{8}$$

where $M_{\Theta,\Phi}(A_\Theta(r))$ is our proposed unfolded deep recursive network.

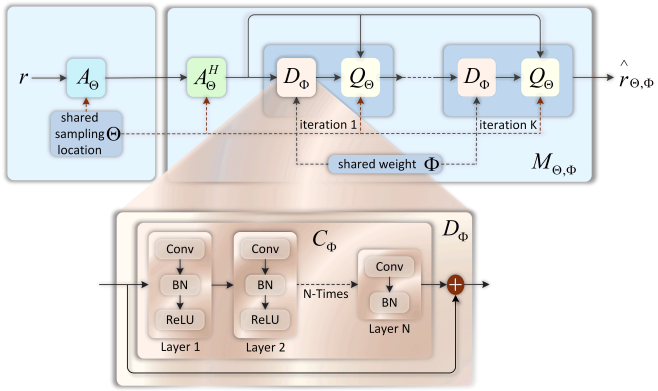

Fig. 1. Optimize network architecture for both sampling and reconstruction

Joint optimization strategy of reconstruction scheme and sampling model: In this paper, we propose a CNN-based framework to jointly optimize the denoising block D_Φ and the data consistency block Q_Θ. Specifically, the following optimization form is used to jointly learn the sampling pattern Θ and the CNN parameters Φ from the training data.

$$\{\Theta^*, \Phi^*\} = \arg\min_{\Theta,\Phi} \sum_{i=1}^{N} \left\| M_{\Theta,\Phi}(A_\Theta(r_i)) - r_i \right\|_2^2, \tag{9}$$

where $r_i, i = 1, ..., N$ are different training images.

Modeling and parameterization of sampling methods: To reduce the trainable parameter size, the two-dimensional sampling locations that need to be trained can be replaced by a combination of two one-dimensional sampling locations. Our approach of reducing dimensionality of the search space by parameterizing the sampling pattern is shown in Figure 2. Specifically, the following forms of sampling patterns are considered.

$$\Theta = \Theta_a \bigcap \Theta_r, \tag{10}$$

where Θ_a and Θ_r are the one-dimensional sampling locations along the azimuth and range directions, respectively. It is assumed here that the readout direction is orthogonal to achieve a full sampling.

It can be seen that the positions $k_{x_i}; i = 1, ..., r$ and $k_{y_i}; i = 1, ..., a$ are the unknown parameters to be trained, and this method can reduce the number of trainable parameters from $a \times r$ to $r + a$, which greatly improves the efficiency of parameter training.

Besides the benefit of reducing the parameter space size, the above approach also simplifies the implementation of the sampling model. Ignore the noise n, the forward model in equation (2) can be transformed according to the Fourier transform as

$$\omega = A_r R A_a^H, \tag{11}$$

where R is a two-dimensional image and A_r and A_a are one-dimensional Fourier transform operators as shown in Figure 2. Sampling operator A_{Θ_r} requires m_r samples in the range direction and A_{Θ_a} requires m_a samples in the azimuth direction, resulting in a total of $M = m_r \times m_a$ samples from $N = P \times Q$ scene cells with a downsampling rate M/N. Here, M is the number of samples collected by the radar system, N is the total number of pixels in the reconstructed SAR image, and P, Q are the number of pixels along the range and azimuth direction of the SAR image, respectively.

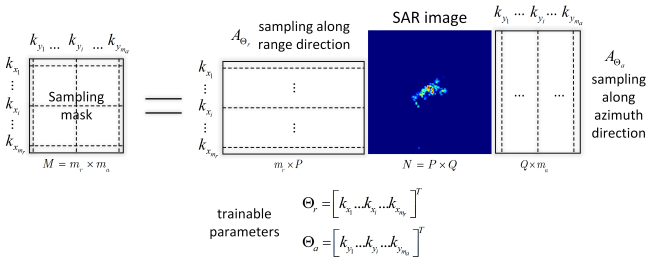

Fig. 2. Diagram of sampling parameterization

It is worth noting that the Fourier transform is computed at the continuous sampling locations k_i and supported by Θ. The Θ and Φ are trained via alternative stochastic gradient descent. In each training iteration, the Φ is firstly fixed and Θ is updated, and then Φ is updated with a fixed Θ. The proposed approach can also improve the efficiency of training iterations by eliminating the need for a non-uniform Fourier transform operator (NUFT).

Experiments and analysis of results: To demonstrate the effectiveness and superiority of the proposed method, we used the MSTAR spotlight SAR dataset [11] to conduct the experiment from a simulated dataset.

The experiments in this paper exploits the deep network shown in Figure 1 with $K = 5$, where K is the number of network layers in Fig. 1. The forward operator A_Θ is implemented by one-dimensional discrete Fourier transform that maps spatial locations to continuous-domain Fourier samples specified by Θ as described in Figure 2. The data consistency block Q_Θ is implemented using the conjugate gradient algorithm with 10 iterations. The CNN block D_Φ is implemented via a UNET with 4 pooling and non-pooling layers and 3×3 trainable filters. The parameters of blocks Q_Θ and D_Φ are then optimized to minimize (9). Since SAR images are complex-valued, all networks are trained using frequency domain complex-valued as input, and training losses are computed on the complex images.

In the experiment, three types of targets (BMP-2, BTR-70 and T-72) are used, where the data with 17° dep. angle are used for training and the data with 15° dep. angle are used for testing. The following is a comparison of the reconstruction results of the proposed method, method described by reference [3] with uniform and random sampling method, and ISTA with uniform and random sampling method under the same experiment setting.

Table 1: Comparison of the PSNR of different sampling schemes

down-sampling ratio	PSNR(dB)				
	uniform sampling (ISTA)	random sampling (ISTA)	uniform sampling (method in reference [3])	random sampling (method in reference [3])	proposed method
75%	37.60	37.72	42.77	43.89	55.11
50%	36.71	37.36	38.70	38.36	51.09
25%	24.15	33.60	27.03	35.16	43.09
12.5%	22.99	26.82	26.32	33.36	38.29

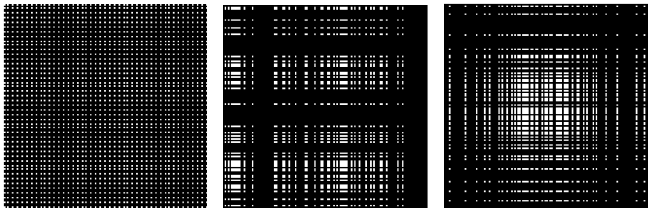

(a) (b) (c)

Fig. 3 *Example of sampling schemes. (a)Uniform Sampling, (b)Random Sampling and (c)Proposed Method.*

Table 2: Comparison of the SSIM of different sampling schemes

down-sampling ratio	SSIM				
	uniform sampling (ISTA)	random sampling (ISTA)	uniform sampling (method in reference [3])	random sampling (method in reference [3])	proposed method
75%	70.08%	70.97%	87.83%	89.39%	99.72%
50%	69.25%	69.47%	76.54%	78.25%	99.53%
25%	48.85%	59.96%	63.00%	71.18%	98.16%
12.5%	26.28%	30.75%	58.03%	70.82%	94.04%

From the experimental results in Table 1 and Table 2, it can be seen that the proposed spotlight SAR imaging method, with jointly optimizing on sampling and reconstruction, maintains high reconstruction accuracy at down-sampling ratios of 75%, 50%, 25% and 12.5%. The peak signal-to-noise ratio(PSNR) of the reconstructed images are all above 38dB, and the structural similarities(SSIM) are all above 94% for our proposed method. The reconstruction accuracy of the method in reference [3] is better than that of ISTA for both uniform sampling and random sampling, but worse than that of the method proposed in this paper. Further more, when uniform sampling is used, although the reconstruction accuracy of both the method in reference [3] and ISTA is better at down-sampling ratio 75% and 50%, it is relatively poor at down-sampling ratio below 50%, which shows that when the sampling rates decrease, the reconstruction performance of uniform sampling also decreases.

The sampling patterns of the proposed method, random sampling method and uniform sampling method are shown in Figure 3. It can be seen that the proposed method samples more densely at low frequencies and more sparsely at high frequencies, which is consistent with the characteristics of the images used in the experiments. The imaging example is shown in Figure 4, it can be seen that the proposed method in this paper retains more details of the targets in the picture compared with reference [3] and ISTA. And when uniform sampling is utilized, the reconstructed images of both methods of reference [3] and ISTA are visually worse.

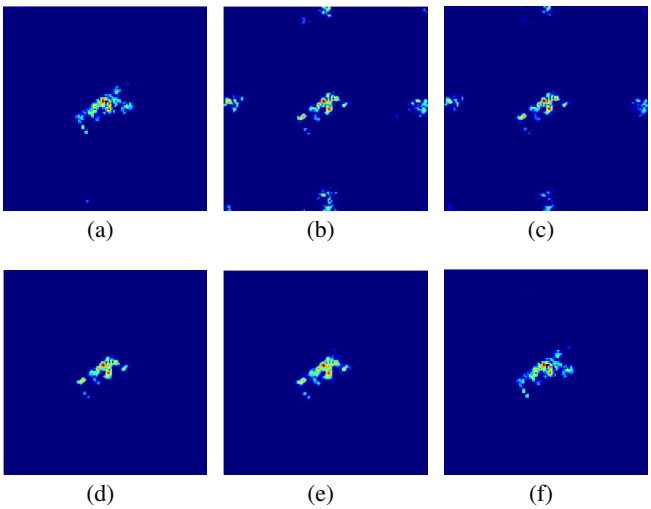

(a) (b) (c)

(d) (e) (f)

Fig. 4 *Example of imaging results and PSNR (down-sampling ratio:25%). (a)Original Image, (b)Uniform Sampling (ISTA) : 24.75dB, (c)Uniform Sampling (Method in Reference [3]) : 26.51dB, (d)Random Sampling (ISTA) : 34.67dB, (e)Random Sampling (Method in Reference [3]) : 37.05dB and (f)Proposed Method : 44.27dB.*

Conclusion: Towards the problems of high computational cost and non-optimized sampling schemes of traditional sparse SAR imaging, this letter proposes a joint optimization method of continuous sampling positions and reconstruction based on deep convolutional neural network. Unlike existing works, we adopt the Fourier operators with continuously defined sampling locations which do not require any approximations to ensure the optimization of the sampling patterns. Experiments based on small data sets in this paper demonstrate the benefits of the proposed joint optimization strategy. Usage of parametric sampling patterns with fewer parameters improves the convergence of the network in the presence of limited size of dataset. Experimental results show that the proposed method has significant advantages in the reconstruction performance.

Acknowledgment: This work has been supported by The National Natural Science Foundation of China (61907008, 61991421, 61991420), The Natural Science Foundation of Guangdong Province (2021A1515012009), AIRCAS grant "Structural sparsity signal high performance adaptive sensing theory and its applications in microwave imaging"

Yao Zhao, Wenkun Huang, and Wing-Kuen Ling (*Guangdong University of Technology, Guangzhou 510006,China*)

Xiangyin Quan (*China Academy of Launch Vehicle Technology, Beijing 100076, China*)

Zhe Zhang (*Suzhou Aerospace Information Research Institute, Suzhou 215123, China; Aerospace Information Research Institute, Chinese Academy of Sciences, Beijing 100190, China*)

Corresponding author: Zhe Zhang (email: zhangzhe01@aircas.ac.cn).

References

1 Zhang, B., Hong, W. and Wu, Y.: 'Sparse microwave imaging: Principles and applications.', *Science China Information Sciences*, 2012, **55(8)**, pp. 1722-1754.
2 Baraniuk, R., and Steeghs, P.: 'Compressive radar imaging.', *IEEE radar conference*, 2007, pp. 128-133.
3 Mason, E., Yonel, B. and Yazici, B.: 'Deep learning for SAR image formation.', *Algorithms for Synthetic Aperture Radar Imagery XXIV*, 2017, **10201**, pp. 1020104.
4 Wang, M., Wei, S., Liang, J., Zeng, X., Wang, C., Shi, J. and Zhang, X.: 'RMIST-Net: Joint range migration and sparse reconstruction network for 3-D mmW imaging.', *IEEE Transactions on Geoscience and Remote Sensing*, 2021, **60**, pp. 1–17.
5 Wei, S., Liang, J., Wang, M., Shi, J., Zhang, X. and Ran, J.: 'AF-AMPNet: A deep learning approach for sparse aperture ISAR imaging and autofocusing.', *IEEE Transactions on Geoscience and Remote Sensing*, 2021, **60**, pp. 1-14.
6 Wei, Y., Li, Y., Ding, Z., Wang, Y., Zeng, T. and Long, T.: 'SAR parametric super-resolution image reconstruction methods based on ADMM and deep neural network.', *IEEE Transactions on Geoscience and Remote Sensing*, 2021, **59(12)**, pp. 10197-10212.
7 Li, M., Wu, J., Huo, W., Jiang, R., Li, Z., Yang, J. and Li, H.: 'Target-oriented SAR imaging for SCR improvement via deep MF-ADMM-Net.', *IEEE Transactions on Geoscience and Remote Sensing*, 2022, **60**, pp. 1-14.
8 Aggarwal, H.K. and Jacob, M.: 'J-MoDL: Joint model-based deep learning for optimized sampling and reconstruction.', *IEEE journal of selected topics in signal processing*, 2020, **14(6)**, pp. 1151-1162.
9 Yang, X., Li, G., Sun, J., Liu, Y. and Xia, X.G.: 'High-resolution and wide-swath SAR imaging via Poisson disk sampling and iterative shrinkage thresholding.', *IEEE Transactions on Geoscience and Remote Sensing*, 2019, **57(7)**, pp. 4692-4704.
10 Knittle, C. D., Doren, N. E. and Jakowatz, C. V.: 'A comparison of spotlight synthetic aperture radar image formation techniques', *Sandia National Lab techreport*,1996.
11 Keydel, E.R., Lee, S.W. and Moore, J.T.: 'MSTAR extended operating conditions: A tutorial.', *Algorithms for Synthetic Aperture Radar Imagery III*, 1996, **2757**, pp. 228-242.